

Received October 23, 2018, accepted November 25, 2018, date of publication December 4, 2018, date of current version December 31, 2018.

Digital Object Identifier 10.1109/ACCESS.2018.2884199

# Remote Sensing: An Automated Methodology for Olive Tree Detection and Counting in Satellite Images

AFTAB KHAN<sup>1</sup>, UMAIR KHAN<sup>1,2</sup>, MUHAMMAD WALEED<sup>1</sup>, ASHFAQ KHAN<sup>3</sup>, TARIQ KAMAL<sup>1</sup>, SAFDAR NAWAZ KHAN MARWAT<sup>1</sup>, MUAZZAM MAQSOOD<sup>2</sup>, AND FARHAN AADIL<sup>2</sup>

<sup>1</sup>Department of Computer Systems Engineering, University of Engineering and Technology, Peshawar 25120, Pakistan

<sup>2</sup>Department of Computer Science, COMSATS University Islamabad at Attock, Attock 43600, Pakistan

<sup>3</sup>Department of Mechanical Engineering, University of Engineering and Technology, Peshawar 25120, Pakistan

Corresponding author: Aftab Khan (aftab.khan@uetpeshawar.edu.pk)

**ABSTRACT** Cultivation of olive trees for the past few years has been widely spread across Mediterranean countries, including Spain, Greece, Italy, France, and Turkey. Among these countries, Spain is listed as the largest olive producing country with almost 45% of olive oil production per year. Dedicating land of over 2.4 million hectares for the olive cultivation, Spain is among the leading distributors of olives throughout the world. Due to its high significance in the country's economy, the crop yield must be recorded. Manual collection of data over such expanded fields is humanly infeasible. Remote collection of such information can be made possible through the utilization of satellite imagery. This paper presents an automated olive tree counting method based on image processing of satellite imagery. The images are pre-processed using the unsharp masking followed by improved multi-level thresholding-based segmentation. Resulting circular blobs are detected through the circular Hough transform for identification. Validation has been performed by evaluating the proposed scheme for the dataset formed by acquiring images through the "El Sistema de Información Geográfica de Parcelas Agrícolas" viewer over the region of Spain. The proposed algorithm achieves an accuracy of 96% in detection. Computation time was recorded as 24 ms for an image size of  $300 \times 300$  pixels. The less spectral information is used in our proposed methodology resulting in a competitive accuracy with low computational cost in comparison to the state-of-the-art technique.

**INDEX TERMS** Remote sensing, olive, Hough transform, crop estimation, satellite imagery, multi-spectral imagery.

## I. INTRODUCTION

Olea Europea, known for its common name as olive, is an evergreen small tree species that belongs to family Oleaceae [1]. The species originates from the Mediterranean as it was first domesticated there about 6000 years ago, spreading to far east China into southern Asia. Today olive is cultivated in each continent around the world [2]. It is one of the most widely distributed crop around the world. Olive oil is the core ingredient of Mediterranean cuisines and is cherished all over the world. Its worldwide distribution makes it an economically significant crop for the countries where it is cultivated. It majorly contributes to the economy of countries like Spain, France, Italy, Greece, Portugal etc. Among those countries, Spain leads the distribution of olive trees cultivated over a land of 2.4 million hectares. Consumption of olives

is showing a significant increase over the past few years and is anticipated to increase by 14 percent in the year 2018 [3].

Production and distribution of such economically significant crop requires a regularized monitoring over the inventories and the crop. It is a critical task for the plantation and resource management. To meet the growing world demand and consumption agricultural output, crop yield must be estimated. Manual collection of crop data for record keeping is humanly infeasible, expensive and susceptible to human error. Latest technology can be employed to achieve this aim.

Remote sensing has presented itself as a reliable and accurate tool for the remote detection and analysis of image data. Over the past few years, advancements in the field of image processing and availability of Very High Resolution (VHR)

images from satellite have led to the automation of several processes [4].

Various techniques and algorithms have been developed for the automatic detection of olive trees. Techniques include the categories of image segmentation [5]–[7], template matching [8], blob detection [9], [10], and supervised learning [11], [12]. Each technique aims at achieving highly accurate detection results. However, they are marred by limitations leaving room for a robust, efficient and effective detection system.

This research work aims at achieving a high accuracy in the detection and recognition of olive trees. The proposed system contributes to the existing work by,

- Developing an accurate and computationally efficient system.
- Testing over diverse image sets with varying ground and environment conditions.
- Achieving high accuracy by utilizing a RGB image reducing the dependency on multi-spectral imagery.

The rest of the paper follows the organization structure as, Section 2 discusses the related work done, and Section 3 presents the methodology of our proposed system. Section 4 covers the experimental setup and results are discussed in Section 5. The paper is concluded along with the discussion of the future work in Section 6.

## II. RELATED TECHNIQUES

Various techniques and algorithms have been devised to detect and enumerate olive trees. These techniques are discussed in the following subsections, grouped by their governing method.

### A. IMAGE SEGMENTATION

Image segmentation is the partitioning of an image into a region of interest and the background information. Required trees were segmented out of the images using thresholding, morphological operations of opening and closing, region growing, edge detection and clustering. These techniques were proposed individually along with a hybrid approach as well.

Chemin and Beck detected and counted olive trees to monitor the loss against the deadly pathogen [6]. *Xylella Fastidiosa* is a bacterial plant pathogen with a wide host range of plants such as grapes, citrus, olives etc. [13]. The study site was chosen over the region of Apulia, Italy. The RGB imagery was captured along with near infrared band by the large photogrammetric cameras. They proposed a multi-staged algorithm consisted of pre-processing of input images, followed by Niblack's thresholding and Sauvola binarization [14] based segmentation. Segmented blobs falling within the parameters of size and area were considered as olive trees. Centroids representing each blob were extracted summing up to give the total number of olive trees. Promising results were obtained from the method

giving an overall mean error of 13 percent. The error was mainly produced due to closely planted trees.

Another algorithm was proposed by Moreno et al. segmenting olive trees from the background soil using k-mean clustering [5]. The algorithm was tested over the RGB satellite imagery acquired by the SIGPAC viewer of Ministry of Environment and Rural and Marine Affairs [15]. The algorithm was tested for varying number of clusters of 2 and 3. Results showed that the algorithm performed significantly better at a lesser number of clusters due to less number of ground information. Results showed an overall omission rate of 0 in 6 samples and a commission rate of 1 in 6 samples. The methodology showed acceptable results but over the less challenging environment and over less number of sample images.

The Joint Research Centre (JRC) [16] developed a tool for the detection and counting of olive trees named as OLICOUNT [7] utilizing various image segmentation techniques such as thresholding, region growing and morphological operation. The tool worked over images with a pixel resolution of 8 bits. However, a later version OLICOUNT v2 was developed to work over images with 16 bits of information per pixel. The integration of 16-bit image support showed no major difference in terms of tool performance [17]. Both developed versions were semi-automatic requiring parameter tuning.

### B. TEMPLATE MATCHING

Template matching is the extraction of the object of interest from the image if it shows a match with predefined models. These models are based on the possible set of images of the object to be detected. The technique is simple yet is limited to the combination of the models.

The plantation of olive trees is done in a reticular pattern with space of 6 to 10 meters between the trees. J. Gonzales utilized the plantation pattern of olive trees and developed a probabilistic model that served as a template to detect and count them [8]. The detection of an olive tree was based on the joint probability of a tree following the reticular pattern along with possessing the characterized geometrical features. These features included size and shape. The reticular pattern was observed by detecting trees at different angles of the neighbourhood to be voted as part of the pattern. A tree satisfying both above constraints was detected as an olive tree. The algorithm was tested over QUICKBIRD satellite imagery over RGB bands, showing an overall detection result of 98 percent. The model used grey-scale version of the images and showed high accuracy, however, offered a few limitations. In the case of irregularly planted trees due to the utilization of space and resources by farmers model showed a downfall in the joint probability. This led to the false count of olive trees.

### C. BLOB DETECTION

In the aerial view, trees show morphological characteristics like blobs. These blobs when looked from above appear

brighter at the tips with shadows following towards their base. Laplacian is a differential operator, mostly used to detect edges along with the detection of blobs [18]. These blob-like structures were detected by Karantzalos and Argyalas using local maxima of Laplacian [9]. Their algorithm was tested over grey-scaled satellite images acquired from the IKONOS and QUICKBIRD satellites. Blob detection is a widely used technique due to its simplicity and robustness, however, is prone to the commission of non-olive data. The technique utilized only circular shaped morphology of trees and considered every object as an olive tree having those characteristics.

Ionis *et al.* proposed a tree counting algorithm as Arbor Crown Enumerator (ACE) [10]. The algorithm was utilized to count olive trees, orange trees and vineyards over Kertis Watershed and Island of Crete. The method was based on a red band Thresholding along with Normalized Difference in Vegetation Index (NDVI) [3] based blob detection. The hybrid technique outperformed previous techniques overcoming the shortcomings of Thresholding and Blob detection when individually applied. Accurate detection and count were observed with an estimation error of 1.3 percent. The algorithm showed accurate results however with the addition of computational cost of multiple bands.

#### D. CLASSIFICATION

An automated olive tree detection method was proposed by Bazi *et al.* [11]. They devised an algorithm utilizing supervised learning techniques to detect and classify olive trees. The method was tested over the agricultural area of Al Jouf in Saudi Arabia. The area was acquired over satellite imagery by IKONOS-2. A Gaussian Process Classifier (GPC) was fed with the feature vectors of objects, morphologically extracted from the satellite imagery. Classification resulted into a binary map of tree and non-tree. The classification results showed an overall accuracy of 96 percent detecting 1124 trees out of 1167. Tree classified components were then counted resulting in a total number of olive trees. The method showed overall accurate results, however, lacked diversity in terms of image number and ground classes. The number of training samples was not enough to evaluate classifier performance accurately.

An object-based classification method was proposed by Peters *et al.* [12]. They detected olive trees over the region of France using a four-step model. The model comprised of image segmentation, feature extraction, classification and result mapping. The model was tested over multi-spectral imagery acquired from various sensors. At each step of the model, synergy methods were developed by combining features from various sensors resulting in an overall accuracy of 84.3 percent.

Another technique was proposed by Moreno *et al.* by using fuzzy logic generating a fuzzy number and utilizing it to detect the olive trees using k-neighbour approach [19]. The methodology was tested over VHR imagery acquired from SIGPAC viewer covering the territory of Spain in

RGB channels. Promising results were obtained from the methodology showing an omission rate of 1 in 6 and a commission rate of 0. Results were generated using the value of  $k$  as 1 and 2. Their technique claimed to be highly accurate, however, the number of testing images and the diversity seemed not enough as per provided information in the literature.

Related work done in the recent years showed the proposition of various techniques and methods to detect olive trees. Techniques from simple image segmentation and blob detection to complex methods of classification have been developed. These techniques utilized satellite images along with the aerially captured images capturing spectral information over grey-scale, RGB and multi-spectral bands. It has been observed that the techniques in literature present high accuracy results but with a few limitations. Publicly available datasets with enough number of images covering diverse cases were not part of the testing images. Algorithms showed an increase in accuracy with an increase in the image spectral information. Some of the proposed techniques left room for improvement due to their proneness towards false detection. They posed challenges of closely planted trees forming joint crowns, varying sizes of trees in an orchard, misaligned plantation of trees to utilize space, and detection and enumeration of trees in complex distribution. These challenges in the existing literature offers enough motivation to propose a technique that focuses on overcoming the above-mentioned shortcomings along with testing it over diverse dataset both in terms of number and ground cover classes. Our proposed system aims at an automated approach of utilizing less image information followed by the efficient and robust processing to reduce the computational cost, resulting in accurate detection and enumeration of olive trees.

### III. PROPOSED METHOD

The overview of the proposed method to detect olive trees is given in Figure 1. The proposed method is a multi-step algorithm utilizing image processing techniques at steps of pre-processing using greyscale converted images and enhancing them using unsharp masking. Followed by the image segmentation through multi-level thresholding leading to the detection of olive trees using circular Hough Transform. Afterwards, trees are counted using the blob analysis technique.

#### A. PRE-PROCESSING

Image pre-processing is the removal of any kind of noise and irregularities present within the image added during the process of its formation [20]. The images during their acquisition from the sensors and optical devices may encounter errors related to geometry and brightness. Images may get blurred due to the motion of optical device or the object itself. Such errors can be removed by statistical and mathematical models. For that purpose, the image is sharpened without increasing the noise. In order to sharpen the edges

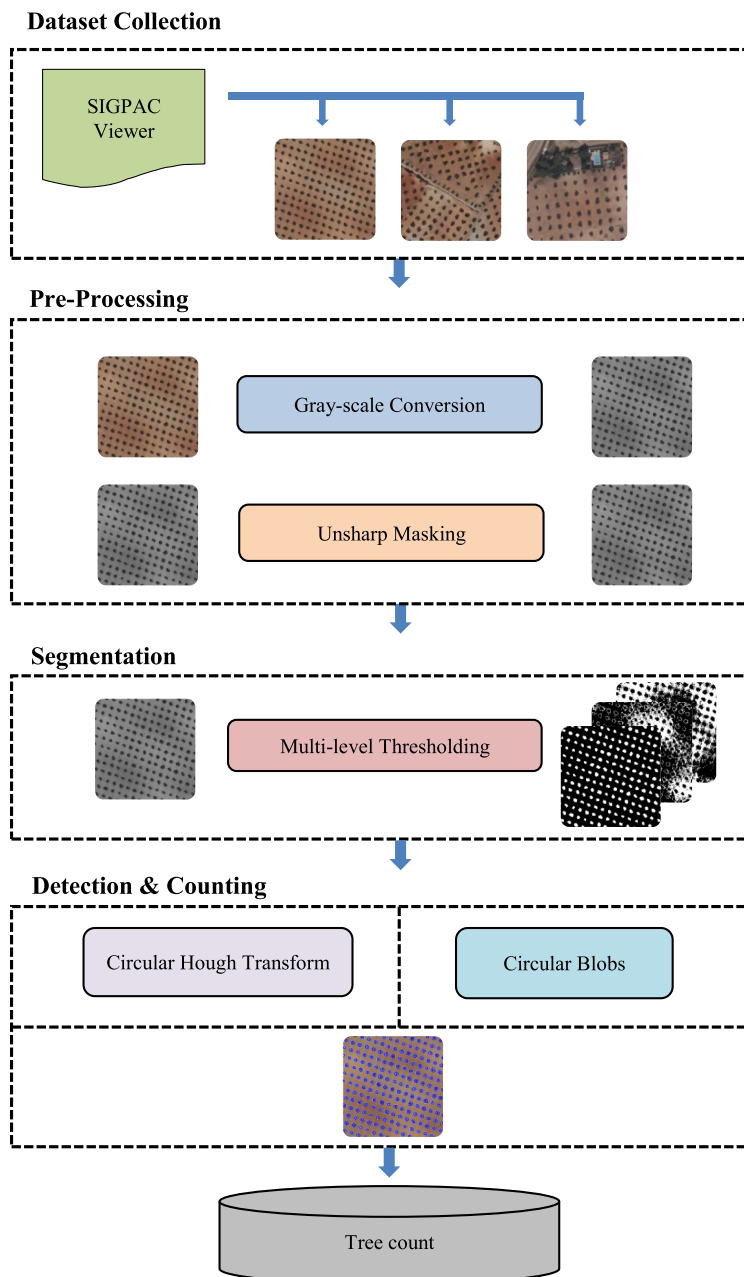


**FIGURE 1. Overview of The Proposed Scheme For Automatic Detection And Counting Of Olive Trees.**

of the image without enhancing the noise, unsharp masking is used [21].

**B. UNSHARP MASKING**

The word “unsharp” is derived from the fact that the sharpening technique uses the blurred and un-sharpened version of the original image as a mask to produce a sharpened resultant image [22]. The flow diagram of the unsharp masking is given as below in Figure 2.

Where,  $f$  is the input image,  $g$  is the resultant difference image between the original image and the smoothed

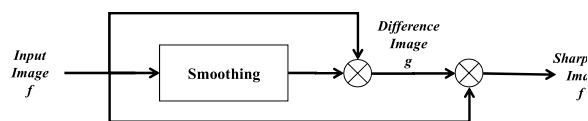


**FIGURE 2. Flow Diagram of Unsharp Masking.**

version of it. The  $f'$  is the result obtained by adding the original image with the enhanced edges.

Unsharp masking filtration over the input grayscale images takes place in following steps.

- Input image  $f$  is smoothed resulting in  $f_{smooth}$  by convolving it with low pass filter  $h$ , removing the sharp varying intensities as given in Equation 1.

$$f_{smooth} = f * h \tag{1}$$

- The smoothed image is then subtracted from the original image giving edges in the result,  $g$ . During the subtraction the low-frequency components are removed leaving the high-frequency components, i.e. edges behind as given in Equation 2.

$$g(i, j) = \sum_{i=1}^M \sum_{j=1}^N f(i, j) - f_{smooth}(i, j) \tag{2}$$

The pixel-wise operation is performed over each pixel location  $i, j$  of the image of size  $M \times N$ .

- The edges are scaled to an appropriate level of sharpness. These edges are then enhanced by multiplying them with a scaling factor  $k$ . The value of  $k$  is based on the amount of sharpness required in the image for further processing. Increasing the value of  $k$ , gives an increase in the amount of sharpness.
- Scaled edges are then added to the original image resulting in an enhanced image,  $f'$  as given in Equation 3.

$$f'(i, j) = \sum_{i=1}^M \sum_{j=1}^N f(i, j) + k \times g(i, j) \tag{3}$$

Stepwise filtration is performed over the input grayscale image which improves the sharpness.

### C. IMAGE SEGMENTATION TECHNIQUES

Image segmentation is the division of the image into subsequent disjoint regions formed by pixels of same intensity levels. Objects are formed into a spatially contiguous group of pixels [16]. Such objects are then further used for higher level processes such as feature extraction, classification and in our case object recognition. In our work, the pre-processed images are taken as an input with multiple ground classes. Each class is represented by a different set of intensity levels. The image is segmented based on those individual levels.

#### MULTI-LEVEL THRESHOLDING – IMPROVED OTSU’S METHOD

Thresholding is one of the major techniques used for the segmentation of input images. Segmentation is mainly done based on the information carried by the histogram. Selection of multiple thresholds is very crucial as accurate results are based on the adequate computation of the threshold values [23]. The criteria for selecting the threshold values for segmentation can be different. Based on the objective function of the thresholding method, criteria for threshold selection is defined. Among the different techniques, we have utilized Otsu’s thresholding method with a few improvements [24].

Otsu’s method is based on the maximization of intra-class variation or the minimization of inter-class variation.

It is a widely used algorithm for segmenting images in binary classes. However, the algorithm can be extended over multiple classes. The concept is based on the selection of multiple threshold values maximizing the difference among the existing classes in the image. The number of thresholds can be either selected manually or through some heuristic approach. Considering an input image,  $I$  represented in  $L$  number of grey-scale levels, with total number of pixels as  $N$ , the number of thresholds is determined through number of peaks in their histogram. The variation in the frequencies of intensity levels produces variation in the histogram in the form of peaks. These peaks are determined by detecting the abrupt change in the frequency distribution graph. The histogram of image with  $b$  number of bins, number of peaks are determined for the variation between the consecutive frequency bins fulfilling the criteria given in Equation 4 as,

$$|b(i) - b(i + 1)| \geq md - md' \tag{4}$$

The change in consecutive frequencies of intensity levels  $i$  and  $i + 1$  greater than the threshold results in the formation of a peak.

Here  $md$  is the mean distribution of maximum intensity levels  $M$  over the pixels  $N$ , and  $md'$  is the mean distribution of contributing intensity levels  $M'$  in image. Both values are calculated as given in Equation (5,6),

$$md = \frac{N}{M} \tag{5}$$

$$md' = \frac{N}{M'} \tag{6}$$

The number of pixels having a grey level  $i$  are given as  $f_i$ . The probability of a pixel in the total of  $N$  pixels having a level  $i$  is given in Equation 7 below,

$$p_i = \frac{f_i}{N}, \quad p_i \geq 0 \tag{7}$$

The cumulative probability of pixels belonging to a class is also calculated in Equation 8 as,

$$\omega_k = \sum_{i=t_{k-1}+1}^{t_k} p_i \tag{8}$$

Where  $p_i$  is the set of all the intensity values in between the range of the two successive thresholds  $t_{k-1} + 1$  and  $t_k$ . The mean grey level for each segment  $k$ , is calculated in Equation 9 as,

$$\mu_k = \sum_{i=t_{k-1}+1}^{t_k} \frac{ip_i}{\omega_k} \tag{9}$$

Using the above equations mean grey level of the entire image and the variance is calculated in Equation (10,11) as,

$$\mu_T = \sum_{k=0}^{k-1} \mu_k \omega_k \tag{10}$$

$$\sigma_B^2 = \sum \omega_k \mu_k^2 - \mu_T^2 \tag{11}$$

Otsu's method focuses on selecting the optimal thresholds maximizing the inter-class variance. It is given in Equation 12 below,

$$\{t_0^*, t_1^*, \dots, t_{k-2}^*\} = \max\{\sigma_B^2(t_0, t_1, \dots, t_{k-2})\} \quad (12)$$

#### D. DETECTION AND COUNTING

Otsu's based thresholding results in a binary image containing olive trees along with the other ground classes. Trees from the aerial view are represented in the form of circular blobs. Binary resultant image from the thresholding technique comprises of both the olive trees along with other ground components with similar intensities. Such components can be filtered out using the Circular Hough Transform (CHT). The CHT works by exploiting the circular geometry of the foreground components of the binary image. The circular blobs over the possible range of radii are thus marked as the olive trees.

##### CIRCULAR HOUGH TRANSFORM (CHT)

Hough transform is a feature extraction technique used to find the objects in an image from a class of shapes [25]. The determination takes place by a voting procedure. CHT is a specialized form of Hough Transform used to determine the circular objects in an input image.

A circle is represented by its centre points along with the radius around which the circle is drawn represented by  $a$ ,  $b$  and  $r$  respectively. The accumulator is a 3-D matrix formed to determine the intersection points in the parameter space. The algorithm is an iterative process that determines the points intersecting with varying values of space parameters. A pixel intersecting the points at centre points and radius results in an increase in the count by 1. The stepwise algorithm is given as below,

- Initialization of Accumulator array  $A [a,b,r]$  by 0.
- Determine the edges in the image using Canny edge detection algorithm.
- Vote the possible circles in the 3-D matrix,  $A$ .
- Find the local maxima in the accumulator  $A$  for  $a$ ,  $b$ , and  $r$ . The maximum votes for the given parameters give the circle.

Circles formed by the intersection of points in the Hough space is shown in Figure 3 below.

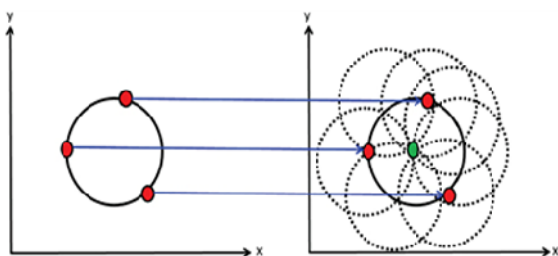


FIGURE 3. Circular Hough Transform for detection of circles in images.

**Algorithm 1 Olive Tree Detection;** Take Satellite Image, Perform Segmentation and Count the Circular Blobs

**Input:** RGB image; kernel;  $k$ ;  $T$ ; ground labels; marked ground truth data

**Output:** Olivemap; olivecount; accuracy

```

1: Procedure UnsharpMasking(img, kernel, k)
2:  $im_{smooth} = \text{lowpass}(img, kernel)$ 
3:  $im_{diff} = im_{smooth} - img$ ,
4:  $im_{sharp} = img + Im_{diff} * k$ 
5: return  $im_{sharp}$ 
6: end procedure
7: procedure OtsuThresholding (imsharp, T)
8:    $(t_0, t_1, \dots, t_T) = \text{thresholds}(im_{sharp}, T)$ 
9:    $(cluster1, cluster2, \dots, clusterT) =$ 
   thresholding(imsharp,  $(t_0, t_1, \dots, t_T)$ )
10: return (cluster1, cluster2, ..., clusterT)
11: end procedure
12: Procedure Detection&Counting (segment,  $r_{min}$ ,  $r_{max}$ )
13:    $(c_n, r_n) = \text{CHT}(\text{segment})$ 
14:   while  $i$  is less than  $n$  do
15:     if  $r_i$  is greater than  $r_{min}$  and less than  $r_{max}$  then
16:       olivecount = olivecount + 1
17:       olivemap = drawcircle(segment,  $c_i$ ,  $r_i$ )
18:     end
19:   end
20: accuracy = 100 - Estimationerror(ground labels,
   ground truth data, olivecount, olivemap)
21: return (olivecount, olivemap, accuracy)
22: end procedure

```

The technical structure of proposed algorithm is shown in the form of pseudocode in the Algorithm 1 below.

#### IV. EXPERIMENTAL SETUP

This section discusses the data used for the evaluation of our proposed scheme. It also briefly discusses the metrics used to evaluate the performance of our algorithm.

##### A. DATASET

To evaluate the performance of our proposed algorithm, images are acquired from the SIGPAC viewer of Ministry of Environment and Rural and Marine Affairs Spain [15]. The viewer provides the satellite imagery from over 16 Spanish communities. Among those communities is the Castilla La Mancha, famous for its vineyards, mushrooms and olive plantations [26]. The community covers the regions of province Toledo known for the high concentration of olive trees. Sample images of size  $300 \times 300$  pixels from those regions are taken from the SIGPAC viewer. These images capture the aerial information of Spanish territory with a spatial resolution of 1 meter in the visible spectrum with bands of Red, Green and Blue. Images from the SIGPAC viewer are taken covering ground classes in various possible arrangements.

Ground classes include olive trees, houses, roads, shrubs and bushes, sparse vegetation and soil with varying contrast distribution. Dataset comprises of a total of 95 images with varying distribution of ground classes adding diversity in terms of number of images along with the ground classes. For each image, olive trees are marked providing the ground truth information for the performance evaluation purposes. Furthermore, to ensure the sound formation of the dataset following criteria has been followed.

- The sampling of each image originates from different coordinates covering ground classes at different views and angles.
- Images capture parts of ground information along with the ground classes.
- Images are kept uniform in terms of dimensions and distribution of ground classes to avoid class imbalance problem.

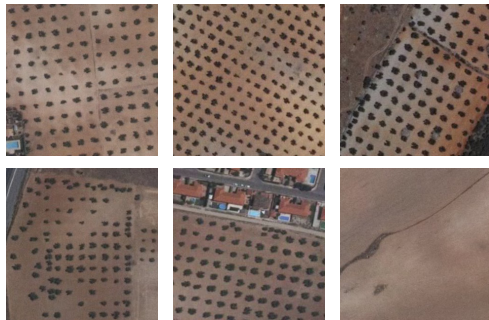


FIGURE 4. Sample images from the test dataset.

Figure 4 presents some sample images from the dataset utilised in this research work.

**B. ACCURACY ASSESSMENT**

To evaluate the performance of our algorithm over the diverse dataset various performance metrics were used and calculated [27]. Each of the metrics is briefly discussed in the section below.

- **Overall Accuracy:** It is defined as the percent olive trees correctly detected with respect to the total number of olive trees present. It gives the number of trees correctly identified among the marked ones in the ground truth information. Mathematically overall accuracy is calculated given in Equation 13 as,

$$Overall\ Accuracy = \frac{No\ of\ Olive\ Trees\ Detected}{Total\ No\ of\ Olive\ Trees} \quad (13)$$

- **Omission Error Rate:** It is defined as the rate with which the positive test subjects are considered as the negative ones. It is the rate at which olive trees are omitted by our proposed system to be detected as olive trees. It is also called a false negative rate. Mathematically, it is presented by Equation 14 as,

$$Omission\ ErrorRate = \frac{Omitted\ Olive\ Trees}{Total\ Olive\ Trees} \quad (14)$$

- **Estimation Error:** It is defined as the difference between the amount of estimated information and the actual information to be estimated. In terms of our proposed system, it is the ratio of the difference between the estimated number of olive trees and actual trees to the actual number of olive trees in the sample. Mathematically in Equation 15, it is given as,

$$Estimation\ Error = \frac{N_{estimated} - N_{actual}}{N_{actual}} \quad (15)$$

Where  $N_{estimated}$  is the estimated number of trees or detected trees and  $N_{actual}$  is the actual number of trees.

**V. RESULTS AND ANALYSIS**

In our proposed olive tree detection algorithm images acquired from the SIGPAC viewer undergo the process of pre-processing. Noise added during the formation of images is removed through filtering. In our proposed system unsharp masking is utilized with a mean filter of size  $3 \times 3$  with  $k$  set as 0.7. Enhanced and sharpened images in the result of pre-processing are shown in Figure 5.

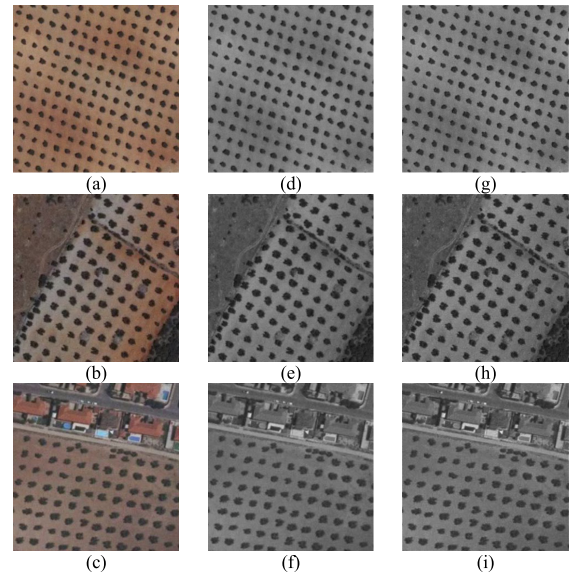
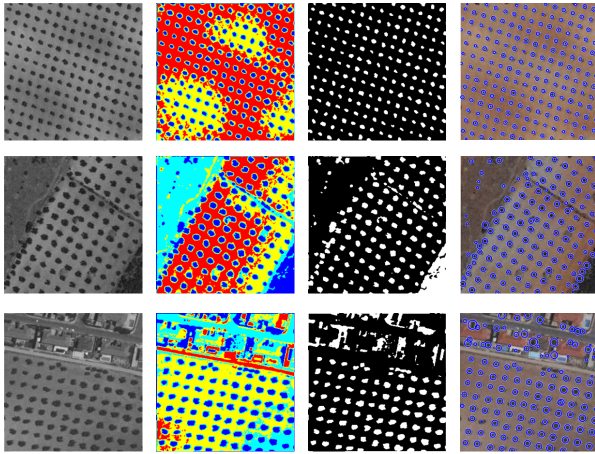


FIGURE 5. Pre-Processing Results (First column shows the original RGB images, second column shows the corresponding grey-scaled version of those images, third column shows the sharpened version.

After the pre-processing of the images region of interest (ROI) was extracted. Image segmentation technique is utilized for this step. Among the image segmentation techniques, threshold-based segmentation is one of the simplest technique of dividing an image based on intensity levels. For a binary segmentation of an image global thresholding is performed by finding the optimal value among the grey-levels of the entire image, however, for multi-level thresholding, multiple local thresholds are selected. In our olive tree detection problem multilevel thresholding using Otsu’s method was performed over 4 levels. Results from image segmentation and olive tree detection are shown in Figure 6.



**FIGURE 6.** Segmentation Results (First column shows the sharpened images, second column represents the multiple segments represented by multiple colors, third column shows the binary segment of olive trees, fourth column shows the detection map).

The segmentation accuracy of a system is measured by calculating the overlapping percentage between the segmented image and the ground truth information. This is measured through Intersection over Union or Jaccard Index. Considering a segmented image,  $A$ , and the ground truth image  $B$ , the Jaccard Index of similarity is calculated as given in Equation 16,

$$J(A, B) = \frac{|A \cap B|}{|A \cup B|} \quad (16)$$

The overall segmentation accuracy of our system came out to be 0.91 showing about 91% of overlap between the segmented output and the ground truth information.

Once the images undergo the multi-level thresholding and olive trees were extracted, other ground components sharing the same intensity levels as of the olive trees became a part of segmentation results thus needing further filtering for accurate detection. Circular Hough Transform was applied over the segmented images filtering out circular blob-like objects with the proposed range of radii. Images over the entire dataset were tested through our proposed system and an overall detection accuracy of 96 percent was achieved.

Detection results over the dataset have been classified among the categories of best and average. Each category of results is discussed and analysed separately.

#### A. BEST CASE SCENARIOS

This included a subset of images from our dataset showing an overall detection accuracy of 100 percent. Images showing 100 percent detection results include cases where olive trees were planted following their distinctive reticular pattern with no other ground class. Those images presented different views of olive tree plantations from different coordinates and regions within the dataset. The detection map of sample input images is shown in Figure 7.

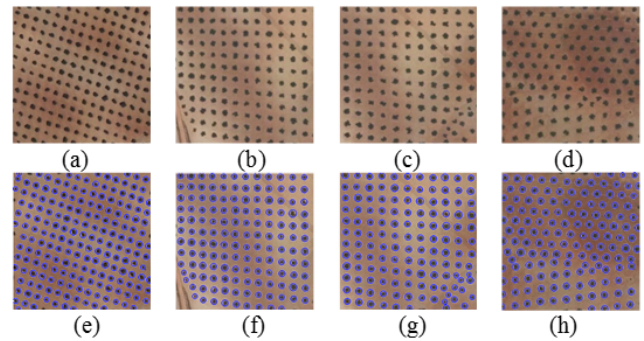


**FIGURE 7.** Best detection results (First row shows original images while second row shows corresponding detection results).

Figure 7(a-c) presents the olive trees planted in a reticular manner with slight variations in angle. The trees were well separated and followed their distinct arrangement in Figure 7(a-b), however, in Figure 7(c) the area in the south-east corner shows the utilization of space by planting trees in a proximity bringing the trees together. Similarly, in Figure 7(d) intersection of olive trees within a field is observed. The trees were planted separately with significant distance in between, however, the trees planted at different angles were intersected at the mid-plane of the field decreasing the distance between the planted trees.. Proposed algorithm accurately detected and enumerated all the olive trees correctly.

#### B. GENERAL RESULTS

The inclusion of other ground components in the sample images resulted in detection accuracy of 95 percent. A few samples from images falling in the average result category are shown in the figure below. Figure 8(a-b) presents the plantation of olive trees along with the sparse vegetation, roads and houses in between. The image shows a hybrid distribution of trees having significant distance among olive trees and closely planted ones. Our proposed algorithm detected almost all the trees, however, considered the young and closely planted trees as one leading to a false count.

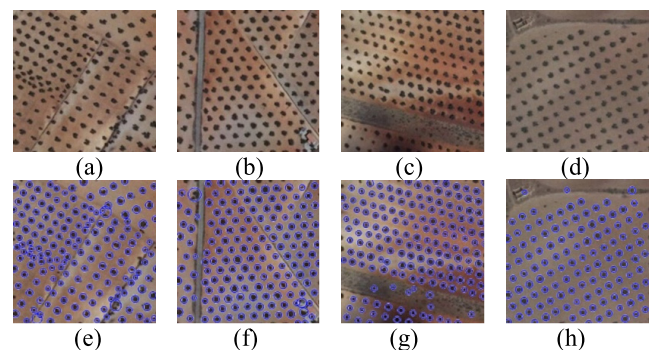


**FIGURE 8.** Average detection results (First row shows original images while second row shows corresponding detection results).



In Figure 8(c) the olive tree plantations were separated by a patch of land in between. The land bears few shrubs and small bushes. Proposed algorithm detected all the trees planted separately along with those in close vicinity. The algorithm showed a 100 percent detection of trees with falsely detecting the shrubs and bushes as young olive trees. The proposed range of radii for the detection of olive trees caters to young olive trees to grown ones. This resulted in the commission of speckles of bushes, rocks and patches of uneven land as olive trees.

In Figure 8(d), olive trees were aligned in their reticular pattern and were well spaced. The image presented the olive trees of almost uniform sizes, however contained other ground components like roads, varying contrasts of soil, bushes etc. Proposed algorithm detected all the olive trees. However, similar intensity levels shared by ground information to that of olive trees added the possibility to be detected when formed varying sized segments. This formation of segments of non-olive information led to the false detection of olive trees and resulting in the false count.

Dense vegetation around the corners formed blob-like structures which were falsely detected as olive trees. On the other hand, closely planted young trees are considered as one leading to the omission of the olive trees. This lead to the false olive tree count. Considering the rest of the images with low detection accuracy the overall detection accuracy of our system came out to be 96 percent.

Image-wise analysis has been made comparing both the segmentation and detection accuracy of each of the image in the dataset through accuracy graph as shown in Figure 9. According to the figure about 70 to 80% of the images showed almost same accuracy for both segmentation and the detection.

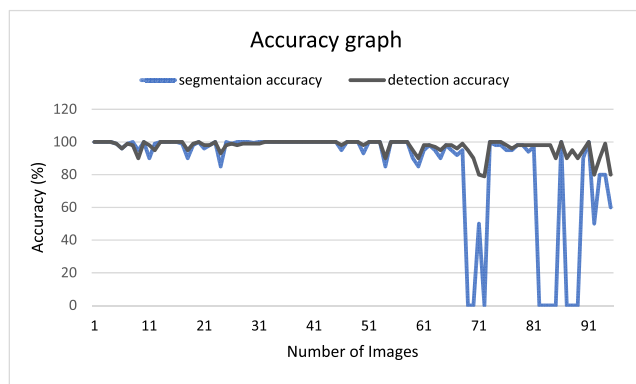


**FIGURE 9.** Image-wise accuracy graph for both segmentation and detection of olive trees.

Variation in the rest of the images is mainly due to the segmentation of non-olive components in comparison to ground truth information resulting in 0% segmentation accuracy. Images showing variation in ground intensities resulted in the formation of large non-olive segments in the segmentation results. Large resultant segments with non-circular uneven geometry were filtered through the CHT in the detection step.

**TABLE 1.** Comparative analysis of the proposed scheme with and without pre-processing.

System	Average Computational Time (ms)	Average Detection rate (%)
Proposed system without pre-processing	22	95
Proposed system with pre-processing	24	96

Removal of resulting segments due to relatively low segmentation accuracy in the detection results provided an overall high detection accuracy.

### C. COMPARISON OF RESULTS WITHOUT PRE-PROCESSING

The proposed methodology is tested over pre-processed images however, a comparative analysis is drawn between the detection accuracy of our methodology with and without the step of image pre-processing as given in Table 1. The unsharp masking consists of consequent steps of image smoothing, followed by the differencing of the images, and addition of the difference with the original image. The aim of the comparative study is to present the results of our proposed system with and without the pre-processing step using CPU implementation [28]. The relationship between the time taken by the two methodologies and their effect on the detection accuracy will help to establish the ground for the need of pre-processing.

The time taken by our proposed method with and without the use of pre-processing is listed in the table below. The difference in the time taken by both the methods is very less as compared to the difference in the detection accuracy of the two methodologies.

The decrease of 1% in the detection accuracy is due to the omission of olive trees that are either young or having low contrast in comparison to their background. Without the pre-processing stage low variations between the different ground components are not enhanced thus leading to some of the trees as undetected. The cumulative image-wise computational time (CT) analysis of our algorithm with and without the pre-processing stage is shown in Figure 10.

### D. COMPARISON WITH STANDARD K-MEAN

K-Mean clustering is another algorithm mostly used for the extraction of foreground information from the background based on the variation among the intensity levels. It works by initializing K number of centroids around which the pixels are clustered forming K number of non-overlapping segments. This iterative process is repeated till the centroids converge to their final position. K-Mean clustering is performed in the segmentation stage of our algorithm resulting in almost similar segmentation results. However, the number of iterations it takes to position the centroids adds an extra computational complexity increasing the computational time (CT) of the algorithm. An image-wise cumulative computational

TABLE 2. Comparative analysis of the proposed scheme vs. benchmark schemes.

Sr. No	Technique	Dataset	Spectrum	Performance Evaluation			
				Overall Accuracy	Commission Rate Error	Omission Rate Error	Estimation Error
1	Proposed Methodology	SIGPAC Viewer	Grey-scale	96%	3 in 100	3 in 100	1.2%
2	Reticular matching [10]	Quickbird	Grey-scale	98%	5 in 100	7 in 100	1.24%
3	Laplacian Maxima [12]	Quickbird/IKONOS	Grey-Scale	N/A	N/A	N/A	N/A
4	GPC[15]	IKONOS-2	RGB	96%	N/A	N/A	3.68%
5	K-mean Clustering [8]	SIGPAC Viewer	RGB	N/A	0 in 6	1 in 6	N/A
6	Fuzzy logic [14]	SIGPAC Viewer	RGB	N/A	0 in 6	1 in 6	N/A
7	Red band Thresholding + NDVI + blob detection [11]	Quickbird	4-bands	N/A	N/A	N/A	1.30%
8	Counting Olive Trees in Heterogeneous Plantations[7]	Acquired Aerial Images	4-bands	N/A	N/A	N/A	13%
9	Synergy of VHR optical and radar data for object-based olive grove mapping[13]	Multisensor imagery	4-bands	84.30%	N/A	N/A	N/A

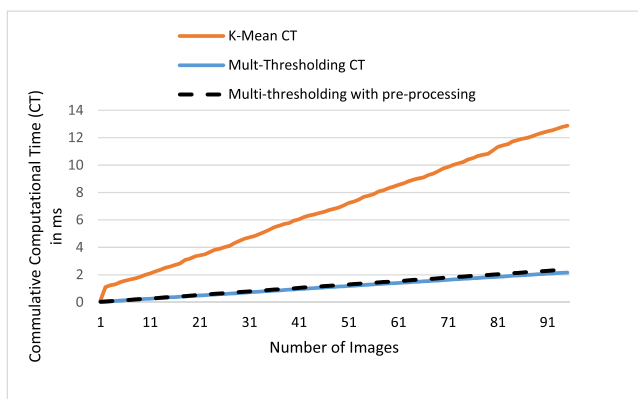


FIGURE 10. Image-wise cumulative computational complexity for utilization of segmentation techniques of K-Mean, Multi-thresholding, Multi-thresholding without pre-processing.

time (CT) graph shows the comparative analysis of our algorithm with segmentation techniques of Multi-thresholding and K-Mean clustering.

E. COMPARISON WITH BENCHMARK SCHEMES

The proposed methodology is compared with the existing techniques and algorithms devised for the automated detection of olive trees. Comparison of the techniques was drawn

based on the evaluation metrics and parameters. Comparison of our proposed methodology with the existing techniques is represented in Table 2. Gonzales [8] proposed an algorithm to detect olive trees by exploiting the reticular pattern in which they are planted. The algorithm was evaluated over the satellite imagery acquired by the Quickbird satellite. The technique was tested over three images with promising detection results with an overall accuracy of 98 percent. However, the algorithm showed its limitation of detecting olive trees in a reticular formation only. Farmers may plant their trees to utilize space and resources which makes the olive trees likely to be omitted.

Karantzos et al. proposed a two-staged detection algorithm consisted of pre-processing followed by the detection of olive trees as local maxima of Laplacian [9]. The algorithm was tested on images acquired from the Quickbird satellite with no performance measures and statistical data provided for evaluation purposes. Yaqub et al. proposed a classification system to detect and count the olive trees in the region of Saudi Arabia [11]. The algorithm comprised of classifying objects using GPC in the image based on their morphological features extracted through operators of opening and closing. The algorithm showed an overall accuracy of 96 percent however, the training and testing data required more samples for

better results. In contrast to the classification model, unsupervised learning was performed by Juan Moreno et al. over the satellite imagery acquired through SIGPAC viewer [5]. The technique was tested and showed promising results, however, the mentioned images did not exhibit diversity in terms of the number along with the utilized ground components.

Ionis et al. devised an algorithm to detect the trees along with their count using the (ACE) [10]. The method utilized the thresholding based on the red band followed by the NDVI values of the multi-spectral imagery. The technique utilized blob analysis for enumeration purposes giving promising results with estimation error up to 1.3 percent. Low error at the high cost of computation over the multiple bands of information made the technique expensive in the computational terms.

Jan Peters et al. proposed an algorithm that developed synergy models based on the four-step classification method [12]. The algorithm classified the VHR images accompanied with the radar data. The classification results showed an accuracy of 84.3 percent. The algorithm utilized the multi-spectral imagery along with the radar data adding computational complexity to the system.

Chemin et al. [6] proposed an algorithm to detect and count olive trees to monitor the significant loss of olive plantations in hands of a deadly pathogen. The images were taken by camera sensors mounted on a drone as part of the campaign. The algorithm detected and counted the olive trees by applying binary thresholding over the input images followed by the localization of centres of blobs. Algorithm showed an estimation error of almost 13 percent. Algorithm considered the diversity of images in terms of sizes, age and density of olive trees however, no information was given regarding the inclusion of other ground data in images.

In comparison to the existing techniques our proposed algorithm utilized least amount of information possible for efficient and robust detection of olive trees. The algorithm was tested over the images acquired from the SIGPAC viewer. The dataset was formed incorporating diversity in terms of number and ground classes. The dataset comprised of over 95 images covering different angles, views and coordinates of the regions of province Toledo, Spain.

The images acquired also included non-olive ground classes including sparse vegetation, shrubs and bushes, soils of varying contrasts, roads, houses and barren lands. The dataset utilized the balanced distribution of these classes to achieve fair results. Our methodology utilized the least information to process, working on 8bits of information per pixel.

Our algorithm utilized the fast and robust thresholding method to segment the foreground information. The proposed system for olive tree detection resulted in an overall accuracy of 96 percent at an average computational time of 24 milliseconds per image of  $300 \times 300$  pixels.

## VI. CONCLUSIONS

In this paper, we have proposed an algorithm to automatically detect and count the olive trees in satellite images.

The proposed methodology is a multi-step algorithm comprising of image processing techniques. The algorithm worked on grey-scale images acquired from the SIGPAC viewer. About 95 sample images were created from the regions of the Toledo, province of Spain. The images were pre-processed using the unsharp masking suppressing the noise present in the image while enhancing the edges for the segmentation process. The segmentation of processed images is performed using the multi-level thresholding utilizing Otsu's method. The segmentation results in the formation of foreground information as the individual segments.

Exploiting the circular geometry, circular blobs among those segments were filtered out using the CHT and counted. Our algorithm detected almost all the olive trees with an overall accuracy of 96 percent. The algorithm showed a few shortcomings of not being able to filter out non-olive tree components falling in the range of radii and exhibiting circular morphology. Also, it did not incorporate the features specific to the olive trees, making it functional for other trees. As future work, we will be incorporating more features of olive trees for accurate detection. We will be using a classification model to reduce the inclusion of non-olive trees in the tree count. We will also be looking forward utilizing the color spectrum to utilize the color information of olive trees.

## ACKNOWLEDGMENTS

The authors would like to thank all the reviewers in helping us improve the quality of our research work draft through their valuable advice and efforts.

## REFERENCES

- [1] H. F. Rapoport, A. Fabbri, and L. Sebastiani, "Olive biology," in *The Olive Tree Genome*. Cham, Switzerland: Springer, 2016, pp. 13–25.
- [2] G. Calabrese, N. Tartaglini, and G. Ladisa, "Study on biodiversity in century-old olive groves," CIHEAM-Mediterranean Agronomic Institute of Bari, Bari, Italy, Tech. Rep., 2012.
- [3] G. Filippa et al., "NDVI derived from near-infrared-enabled digital cameras: Applicability across different plant functional types," *Agric. Forest Meteorol.*, vol. 249, pp. 275–285, Feb. 2018.
- [4] P. Srestasathien and P. Rakwatin, "Oil palm tree detection with high resolution multi-spectral satellite imagery," *Remote Sens.*, vol. 6, no. 10, pp. 9749–9774, 2014.
- [5] J. Moreno-Garcia, L. J. Linares, L. Rodriguez-Benitez, and C. Solana-Cipres, "Olive trees detection in very high resolution images," in *Proc. Int. Conf. Inf. Process. Manage. Uncertainty Knowl.-Based Syst.*, 2010, pp. 21–29.
- [6] Y. H. Chemin and P. S. Beck, "A method to count olive trees in heterogeneous plantations from aerial photographs," 2017.
- [7] A. K. Ramanikaran, S. C. Manoharan, and R. Swaminathan, "Laplace Beltrami eigen value based classification of normal and Alzheimer MR images using parametric and non-parametric classifiers," *Expert Syst. Appl.*, vol. 59, pp. 208–216, Oct. 2016.
- [8] J. González, C. Galindo, V. Arevalo, and G. Ambrosio, "Applying image analysis and probabilistic techniques for counting olive trees in high-resolution satellite images," in *Proc. Int. Conf. Adv. Concepts Intell. Vis. Syst.*, 2007, pp. 920–931.
- [9] K. G. Karantzas and D. P. Argialas, "Towards automatic olive tree extraction from satellite imagery," in *Proc. 20th ISPRS Congr. Geo-Imag. Bridging Continents*, 2004, pp. 12–23.
- [10] I. N. Daliakopoulos, "Tree crown detection on multispectral VHR satellite imagery," *Photogramm. Eng. Remote Sens.*, vol. 75, no. 10, pp. 1201–1211, 2009.

- [11] Y. Bazi, H. Al-Sharari, and F. Melgani, "An automatic method for counting olive trees in very high spatial remote sensing images," in *Proc. IEEE Int. Geosci. Remote Sens. Symp. (IGARSS)*, Jul. 2009, p. II-125.
- [12] J. Peters, F. Van Coillie, T. Westra, and R. De Wulf, "Synergy of very high resolution optical and radar data for object-based olive grove mapping," *Int. J. Geograph. Inf. Sci.*, vol. 25, no. 6, pp. 971–989, 2011.
- [13] S. Soubeyrand, "Inferring pathogen dynamics from temporal count data: The emergence of *Xylella fastidiosa* in France is probably not recent," *New Phytologist*, vol. 219, no. 2, pp. 824–836, 2018.
- [14] R. Kaur, W. Van Dover Stoecker, N. K. Mishra, and R. Kasmir, "Thresholding methods for lesion segmentation in dermoscopy images," U.S. Patent 15/785 232, Oct. 16, 2017.
- [15] G. Gupta, "Algorithm for image processing using improved median filter and comparison of mean, median and improved median filter," *Int. J. Soft Comput. Eng.*, vol. 1, no. 5, pp. 304–311, 2011.
- [16] H. Costa, G. M. Foody, and D. S. Boyd, "Supervised methods of image segmentation accuracy assessment in land cover mapping," *Remote Sens. Environ.*, vol. 205, pp. 338–351, Feb. 2018.
- [17] S. Bagli, *Technical Documentation Olicount v2*, document IPSC/G03/P/SKA/ska D(2005)(5217), Joint Research Centre, 2005.
- [18] Z. Othman et al., "Comparison between edge detection methods on UTeM unmanned aerial vehicles images," in *Proc. MATEC Web Conf. EDP Sci.*, 2018, p. 06029.
- [19] J. Moreno-Garcia, L. Jimenez, L. Rodriguez-Benitez, and C. J. Solana-Cipres, "Fuzzy logic applied to detect olive trees in high resolution images," in *Proc. IEEE Int. Conf. Fuzzy Syst. (FUZZ)*, 2010, pp. 1–7.
- [20] N. P. Bhosale and R. R. Manza, "A review on noise removal techniques from remote sensing images," in *Proc. Nat. Conf. CMS*, 2012, pp. 1–4.
- [21] K. Zhang, "An image enhancement technique using nonlinear transfer function and unsharp masking in multispectral endoscope," in *Proc. Int. Conf. Innov. Opt. Health Sci.*, 2017, p. 1024504.
- [22] K. Panetta, A. Samani, and S. Agaian, "A robust no-reference, no-parameter, transform domain image quality metric for evaluating the quality of color images," *IEEE Access*, vol. 6, pp. 10979–10985, 2018.
- [23] L. Shen, C. Fan, and X. Huang, "Multi-level image thresholding using modified flower pollination algorithm," *IEEE Access*, vol. 6, pp. 30508–30519, 2018.
- [24] M. H. J. Vala and A. Baxi, "A review on Otsu image segmentation algorithm," *Int. J. Adv. Res. Comput. Eng. Technol.*, vol. 2, no. 2, pp. 387–389, 2013.
- [25] K. Okokpujie, "An improved iris segmentation technique using circular Hough transform," in *Proc. IT Converg. Secur.*, 2018, pp. 203–211.
- [26] C. La Mancha. *Worlds of Flavor Spain*. Accessed: Mar. 10, 2018. [Online]. Available: <http://www.worldsofflavorspain.com/node/494>.
- [27] R. G. Congalton, "A review of assessing the accuracy of classifications of remotely sensed data," *Remote Sens. Environ.*, vol. 37, no. 1, pp. 35–46, 1991.
- [28] J. Senthilnath, S. Sindhu, and S. N. Omkar, "GPU-based normalized cuts for road extraction using satellite imagery," *J. Earth Syst. Sci.*, vol. 123, no. 8, pp. 1759–1769, 2014.



**UMAIR KHAN** is a graduate student of Computer Systems Engineering Program at the University of Engineering and Technology (UET), Peshawar, Pakistan, and a student of the M.S. program in Computer System Engineering with UET. He is currently a Research Associate with COMSATS University Islamabad at Attock. His research concentrates on advanced concepts of image processing and machine learning.



**MUHAMMAD WALEED** received the B.Sc. and M.Sc. degrees from the University of Engineering and Technology (UET), Peshawar, in 2014 and 2017, respectively, where he is currently pursuing the Ph.D. degree in image processing. He did his Intermediate (Pre-Engineering) at the Government College, Peshawar, from 2008 to 2010. He is currently a Teaching Assistant with UET. His research interests include image processing, networking, and data compression.



**ASHFAQ KHAN** received the B.E. degree in mechanical engineering and the M.Sc. degree in advance manufacturing from the National University of Sciences and Technology in 2007 and 2008, respectively, and the Ph.D. degree from Manchester University (UoM), U.K., in 2011. He conducted his Ph.D. research on laser-based micro-/nano-manufacturing and characterization at UoM, by the funding from the University of Engineering and Technology (UET), Peshawar. Soon after his Ph.D., he was a Research Visitor at UoM, where he was able to continue his research work. In 2012, he joined UET as Assistant Professor. He has been an Assistant Professor with the Department of Mechanical Engineering, UET, since 2012. He is the first-ever Ph.D. graduate under UET's Development Project at the Jaloza Campus, UET Peshawar, and has returned before his due time. He is currently the youngest Ph.D. of Khyber Pakhtunkhwa. His laser processing expertise includes processing with pulsed and continuous wave lasers of different wavelengths. His characterization skills include optical microscopy, scanning electron microscopy, transmission electron microscopy, X-ray diffraction, atomic force microscopy, and white light interferometry. His research interests include laser advanced manufacturing, micro-/nano-fabrication, laser-based net shape manufacturing, CNC machining, rapid prototyping, and micro-/nano-characterization.



**TARIQ KAMAL** received the B.Sc. degree in computer system engineering from the University of Engineering and Technology (UET), Peshawar, the M.Sc. degree from The George Washington University, USA, and the Ph.D. degree from Virginia Tech, USA. He is currently an Assistant Professor with the Department of Computer System Engineering, UET. His research interests are in the field of software engineering and high performance computing; specifically, he is interested



**AFTAB KHAN** received the B.E. degree in computer system engineering from the College of Electrical and Mechanical Engineering, National University of Sciences and Technology (NUST), Islamabad, Pakistan, in 2009, the Ph.D. degree in single-image blind deblurring and restoration techniques from The University of Manchester, U.K., in 2014. From 2010 to 2013, he was a Graduate Teaching Assistant with The University of Manchester. He has been an Assistant Professor with the

Department of Computer Systems Engineering, University of Engineering and Technology (UET), Peshawar, since 2013. His image restoration expertise includes restoration of blurred images using blind deblurring techniques based on non-reference image quality measures. His image processing skills include OCT image denoising, medical image analysis, and image fusion. His research interests include digital image restoration, blind image deblurring, medical image processing, and digital image and video compression. He was a recipient of the Faculty Development Scholarship from UET for his Ph.D. research study.



Assistant Professor with UET. His research focuses on machine-to-machine communications and future mobile networks.

**SAFDAR NAWAZ KHAN MARWAT** received the B.Sc. degree in computer systems engineering from the University of Engineering and Technology (UET), Peshawar, Pakistan, in 2006, and the M.Sc. degree in communication and information technology from the University of Bremen, Germany, in 2011. He defended his Ph.D. thesis at the University of Bremen in 2014. He was a Lecturer with the Peshawar College of Engineering, Peshawar, from 2006 to 2008. He is currently an



interests include vehicular ad hoc networks, intelligent transportation systems, and bio-inspired algorithms.

**FARHAN AADIL** received the B.S. degree in computer science from Allama Iqbal Open University, Pakistan, in 2005, and the M.S. degree in software engineering and the Ph.D. degree in computer engineering from the University of Engineering and Technology, Taxila, Pakistan, in 2011 and 2016, respectively. He pursued a career in the computer science from 2005 to 2009. He is currently an Assistant Professor with the COMSATS University Islamabad at Attock, Pakistan. His research

• • •



**MUAZZAM MAQSOOD** received the B.S. degree in software engineering and the M.S. and Ph.D. degrees in software engineering from UET, Taxila, Pakistan, in 2007, 2013, and 2017, respectively. He is currently an Assistant Professor with the COMSATS University Islamabad at Attock, Pakistan. His current research areas are machine learning, image and video processing, and recommender systems.